THEORETICAL AND EXPERIMENTAL STUDY ON GEOMETRY RELATED PHASE-MATCHING CONDITION FOR THIRD HARMONIC GENERATION

Mihai STAFE[1*], Constantin NEGUȚU[1*], Georgiana C. VASILE[1] and Niculae N. PUȘCAȘ[1]

We present a theoretical- analytical and numerical- study on the phase-matching condition for third harmonic (TH) generation by focusing gaussian laser pulses in dispersive non-linear (NL) media. We address the influence of the irradiation geometry on the efficiency of TH generation process. We find that for a fixed length of the NL medium, the intensity of TH signal at the output of the NL medium can be increased by two alternative approaches. First, by focusing the driving laser radiation at the frontier of the NL medium rather than in the center of the NL medium. Second, by increasing the driving beam waist radius while laser intensity is kept constant. Both methods are demonstrated to be successful for increasing the TH signal because they minimize destructive superposition of the TH emissions before and after the focus due to Gouy phase-shift. When the two methods are combined, i.e. loose focusing of the driving laser at the frontier of the NL medium, we can boost the TH signal by more than one order of magnitude as compared to the case of non-optimized irradiation geometry condition. The theoretical results on the dependence of the TH signal to the driving beam waist radius are supported by experimental data.

Keywords: non- linear optics, phase-matching condition, third harmonic generation.

1. Introduction

In the last years, several theoretical and experimental papers concerned the third-order harmonic generation (THG) which has become a leading research field in non-linear (NL) optics as a way to produce coherent ultraviolet radiation, [1]-[8].

Several properties of a material change due to the NL effects which occur when the high power laser radiation, characterized by electric field intensities around $10^6 \div 10^7$ V/cm or higher (which are comparable to the atomic electric field), interacts with the material [1], [9]. The third harmonic (TH) radiation can be

[1] University POLITEHNICA of Bucharest, Physics Department, Bucharest, Romania,
[*] Corresponding authors: constantin.negutu@upb.ro; mihai.stafe@upb.ro

used for various applications such as optical lithography and pump-probe experiments.

The TH pulses is produced by focusing near-infrared laser pulses in gases [1], laser-generated plasmas [8], ablated nanoparticles etc. In isotropic (centro-symmetric) media (e.g. gases), for symmetry reasons only odd harmonics are produced, with efficiencies up to 50%.

The full theory of harmonic generation must include the complete atomic level structure of the target atoms, the nonperturbative interaction of these levels with the intense laser field, the depletion of the neutral atoms due to ionization, the dispersion of the resulting plasma, the geometrical complications resulting from the spatial and the temporal distribution of the field strengths near the focus, and the propagation of the fundamental and the harmonic waves through the perturbed medium.

The paper is organized as follows: in Section 2 we present theoretical considerations and analytical results describing the phase matching condition; in Section 3 we present the theoretical model for numerical calculation of the TH field; in Section 4 we discuss the obtained results concerning several parameters in order to obtain the highest conversion efficiency; in Section 5 we outline our conclusions concerning the results.

2. Theory on phase matching condition

Typically, a particular generated harmonic and the fundamental laser field are matched in phase over distances that are many times the wavelength of the incident light. However, the length over which the harmonic phases are matched (*the coherence length*) can be much shorter than the focal depth (typically, 1 mm) owing to different rates of diffraction for different wavelengths

Because of these issues, it is typical to confine the interaction region to a single geometrical coherence length to avoid destructive phase cancellations (geometrical only). This is usually done by lengthening the laser focus relative to the width of the gas jet or by working outside of the focus. This method does not utilize the high-intensity focal volume outside of the coherence length. After a coherence length, new harmonic production is out of phase with previously generated harmonic light (Fig. 1.) The generation of a particular harmonic can go in and out of phase many times in the laser focus. Harmonic light generated at the first position is out of phase with the harmonic light generated at the second position, but in phase with the light generated at the third position.

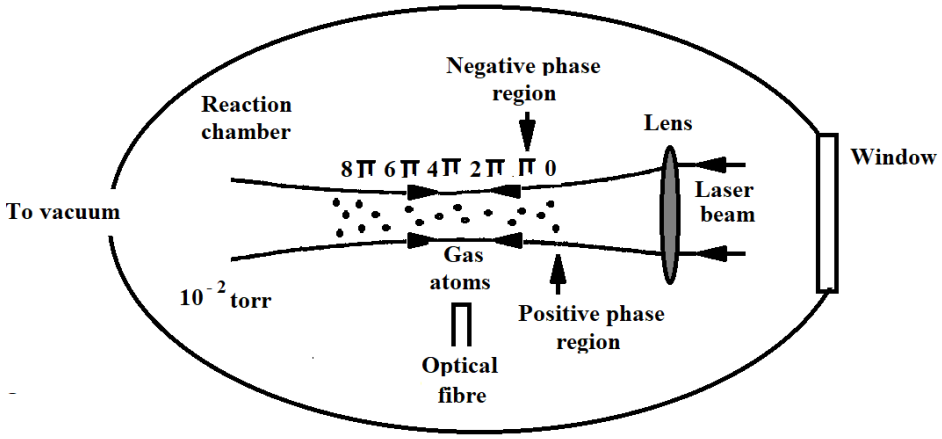

Fig. 1. Phase variation of harmonic emission throughout the laser focus.

Phase mismatches can cause severe destructive interference for harmonic light emerging from different locations in the laser focus. The efficiency of converting the fundamental light into high-order harmonics is limited by several phase mismatch phenomena: 1) the refractive index n for the center fundamental wavelength of the pulse laser light, λ_0 differs from the refractive index for the shorter-wavelength harmonics; 2) the intrinsic phase of harmonic emission can vary longitudinally and radially throughout the focus because of varied atomic response to the local laser intensity; 3) geometrical phase mismatches arise from discrepancies between the diffraction rates for the laser and for individual harmonics.

2.1 Plasma phase mismatches

Since the strongest harmonic emission occurs as atoms undergo ionization by the laser field, we are often interested in harmonic generation in the presence of plasma consisting of free electrons and their parent ions together with the remaining intact neutral atoms. Under typical high-harmonic generation conditions [1,7], if the gas becomes fully ionized, the appearance of free electrons associated with ionization causes the length over which the harmonic phase slips by π relative to the phase of new harmonic production to be as little as few tens of microns.

The coherence length L_c for generating the q-th harmonic in a NL medium with frequency-dependent refractive index can be written in the form:

$$L_c = \frac{\pi}{\Delta k} = \frac{\pi}{qk_0 - k_q} \tag{1}$$

where $\Delta k = \frac{2\pi q}{\lambda_0}\left[n(\lambda_0) - n(\lambda_0 / q)\right]$, k_0 is the propagation vector of the fundamental and k_q is that of the q-th harmonic order. L_c describes the propagation distance between two locations of harmonic emission that are exactly out of phase. In other words, at the end of the coherence length, there is a π phase slip between the fundamental field and the harmonic field that was generated at the beginning of the coherence length [7].

2.2 Neutral gas dispersion

For the dispersion of the plasma, because of ionization, the density of neutral atoms is also scaled by the fraction of ionization, η, giving a phase mismatch between the fundamental and harmonic fields of:

$$\Delta k_N = \frac{2\pi q}{\lambda_0}\frac{P}{P_{atm}}\delta_n(1-\eta) \tag{2}$$

in which $\delta_n = \delta(\lambda_0 / q) - \delta(\lambda_0)$ is the difference in the index of refraction between the fundamental and harmonic wavelengths, and P / P_{atm} is the fractional pressure with respect to atmospheric pressure.

2.3 Plasma dispersion

For the dispersion of the plasma, the phase mismatch is given by:

$$\Delta k_{Pl} = \eta N_{atm} r_e \lambda_0 \frac{P}{P_{atm}}\frac{q^2 - 1}{q} \tag{3}$$

where N_{atm} is the atomic number density at STP and r_e is the classical electron radius. Since $\frac{q^2 - 1}{q} \approx q$ when $q >> 1$, this factor is often approximated for high orders.

2.4 Geometrical phase mismatches

Geometrical phase mismatches gives the phase deviation between a laser wave front that undergoes focusing compared to the phase front of a plane wave, (the laser Gouy shift):

$$\Delta k_G = -\frac{q\lambda_0}{\pi w_0^2} \tag{4}$$

where w_0 is the fundamental beam waist radius (i.e the beam radius in focus) [2].

A phase change of $\Delta\varphi = \pi$ over an approximate coherence length of:

$$\Delta x = \pi x_0 / q \tag{5}$$

is as an estimate for the coherence length of individual harmonics near the center of the laser focus [7], [9]. Here $x_0 = \frac{\pi w_0^2}{\lambda_0}$ is the Rayleigh length.

To reduce geometrical phase mismatches, the depth of focus can be increased relative to the gas jet width to confine the interaction region to a single geometrical coherence length, thus avoiding destructive phase cancellations. However, loose focusing requires greater laser pulse energy to achieve the same intensity. Unfortunately, the high-intensity regions in the beam before and after the single coherence length cannot be utilized in this case.

2.5 Balancing Phase Mismatch. Free Focus

Phase matching for efficient generation of harmonics can be achieved by balancing the various dispersion terms for a zero net phase mismatch. Based on the theoretical model presented in paper [7] in the case of free focusing, the total phase mismatch is given by :

$$\Delta k = \Delta k_N + \Delta k_{Pl} + \Delta k_G = \frac{2\pi q}{\lambda_0}\frac{P}{P_{atm}}\delta_n(1-\eta) + \eta N_{atm} r_e \lambda_0 \frac{P}{P_{atm}}\frac{q^2-1}{q} - \frac{q\lambda_0}{\pi w_0^2} \quad (6)$$

The dispersion of the resultant ions are often neglected for a couple of reasons: first, the resonance frequency is higher than that of neutral atoms, and second, by the time there is a significant population of ions, when $\eta > 0.1$, the free electron contribution to the phase mismatch is much greater than any other term. For the balancing of the total phase mismatch one can use the geometrical phase mismatch, but also the neutral gas dispersion [7].

The intensity of the harmonic light detected at the end of nonlinear medium of length, L depends sensitively on the phase mismatch:

$$I_q = I_q^{\max}\frac{\sin^2(\Delta kL/2)}{(\Delta kL/2)^2} \quad (7)$$

Fig. 2 presents the relative intensity of the TH light (q=3) detected at the end of NL medium (Xe in air) of length L vs the phase mismatch.

Fig. 2. The relative intensity of the third harmonic light vs the phase mismatch for HHG in Xe and air.

As can be seen from Fig. 2, the maximum conversion efficiency is achieved for zero phase, but also for other values of the phase: ±1.45 rad, ±2.42 rad, etc., which are symmetrically concerning the central maximum.

Taking into account the THG for the following parameters [5], [7]: $L_c = 22.23$ μm, $L_{\text{int}} \approx 16.936$ μm, the length of the nonlinear medium which assure an optimal efficiency in Xe in air is $L \approx 5.73$ μm using Nd:Glass laser with wavelength 1.054 μm [5], [7].

3. Theoretical model for numerical calculation of the third harmonic field

We simulated numerically the process of THG by focusing fundamental (F) driving laser pulses with Gaussian intensity profile into a dispersive, homogeneous and isotropic NL medium. We consider that F radiation, at frequency ω, propagates along the *x* axis in the NL medium, being linearly polarized along the *y* axis. We denote the third order susceptibility of the NL medium as $\chi^{(3)}$, the electric field at F frequency ω as $E_{\omega y} + c.c.$, and the electric field at TH frequency (3ω) as $E_{3\omega y} + c.c.$ We neglect the influence of non-linear polarization at the F frequency (describing the optical Kerr effect) on the propagation of the F pulse: $P_{NLy}(\omega) = 0$. The generation of TH radiation in the NL medium through coupling of 3F photons is described by the polarization oscillating at frequency 3ω:

$$P_{NLy}(3\omega) = \varepsilon_0 \chi^{(3)} \left(E_{\omega y}\right)^3. \tag{8}$$

The coupled wave equations describing the propagation of F (q=1) and TH (q=3) radiations within the NL medium can be written in a concise way as follows [11,12]:

$$\nabla\times\left(\nabla\times\vec{E}_q\right)-k_q^2\varepsilon_{rq}\vec{E}_q=\omega_q^2\mu_0\vec{P}_{NL}(\omega_q) \quad (9)$$

where ε_{rq} denotes the frequency dependent dielectric constant of the NL medium.

We used Newton method implemented in COMSOL software to solve numerically the coupled non-linear wave equations for F and TH radiations (9) in the frequency domain (i.e. in stationary conditions), an approximation which is valid for laser pulses as short as ns-ps but not for ultrashort laser pulses such as tens of fs. Due to the symmetry of the problem involving gaussian laser pulses, we chose a 2D (xOy) rectangular domain to solve eqs. (9), with the Ox axis corresponding to the propagation direction of the radiation. The dimensions of the NL medium are L along the axial x direction and h along the radial y direction. The origin of the Ox axis is in the focal plane and the origin of Oy axis is in the center of the F gaussian beam.

Due to the 2D geometry, the Gaussian profile of the F pulse impinging on the front (i.e. left) boundary of the domain, positioned at x=-L/2, is set to "scattering boundary" defined as:

$$E_y(x,y)=E_0\sqrt{\frac{w_0}{w(x)}}\exp\left(-\frac{w^2(x)}{2w_0^2}\right)\exp\left[-\mathrm{i}\left(k_0x+k_0\frac{y^2}{R(x)}-\eta(x)\right)\right] \quad (10)$$

Here, $E_0 \propto \sqrt{I_0}$ is the field amplitude, $w(x)=w_0\sqrt{1+\frac{x^2}{x_0^2}}$ denotes the beam radius at axial x position away from the focus, $R(x)=x\left(1+\frac{x_0^2}{x^2}\right)$ is the position dependent wavefront radius, and $\eta(x)=\frac{1}{2}\mathrm{atan}\left(\frac{x}{x_0}\right)$ is the Gouy phase shift of the Gaussian beam near its waist.

The rear (i.e. right) boundary of the domain, positioned at x=L/2, is also set to "scattering boundary" with no incident field: $\vec{n}\times\left(\nabla\times\vec{E}\right)-\mathrm{i}k\vec{n}\times\left(\vec{E}\times\vec{n}\right)=0$. The lateral boundaries, positioned at y=-h/2 and y=h/2, are set to "perfect electric conductor": $\vec{n}\times\vec{E}=0$.

4. Numerical and experimental results

We present here numerical simulations on the influence of the focusing conditions on the efficiency of THG in Xe. We consider that driving laser beam is a "long" ns-

ps laser pulse at 1064 nm wavelength. The laser is focused to variable beam waist radius $w_0 = (1 \div 10)\,\mu\text{m}$ into the dispersive NL medium (Xe, [10,13]), while the maximum intensity in the focus is kept constant at I_0=10 TW/cm^2.

The dimensions of the NL medium are L=20 μm in the axial Ox direction and h=20 μm in the transverse Oy direction. The 2D spatial mesh is set linear along the axial direction, with a minimum step of 50 nm, and is set denser near the Ox axis in the radial direction with a minimum step of 5 nm. The numerical simulations were carried for $\chi^{(3)} = 10^{-21}\,\text{m}^2/\text{V}^2$.

Fig 3(a) presents the F- field distribution within the NL medium when the F beam is focused to 1 beam waist w_0=1 μm into the center of the NL medium. Typical spatial distribution of the TH intensity across the NL medium is presented in Fig3(b). One can see in Fig. 3(b) that the building of TH radiation is starting before the F focus but is not continuous along the NL medium: it ceases after approximately 6 μm, which is approximately the Rayleigh length of the focal volume, and starts again afterwards. This is due to the dispersion of the NL medium (discussed in Sections 2.1 and 2.2) and the relative values of L and coherence length L_c given by (1). For comparison, we present in Fig. 3(c) the distribution of the TH intensity across the NL medium in case of a non-dispersive NL medium. One can see that the building of TH radiation is continuous from the starting point (which is before the focal plane) across the NL medium.

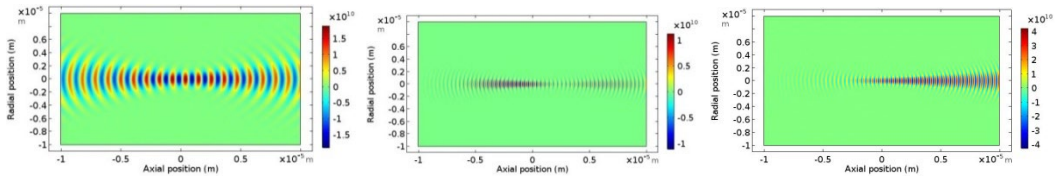

(a) (b) (c)

Fig. 3. 2D plot of the field distribution within the NL medium for (a) F radiation, (b) TH radiation in dispersive NL medium, (c) TH radiation in non-dispersive NL medium

Next, we studied the TH signal at the output boundary as a function of focus position. The influence of the focus position on the TH intensity in the center of the output boundary is presented in Fig. 4(a), while the influence on the TH flux on the output boundary is presented in Fig. 4(b). One can note in Fig 4(a) that the best condition to get most intense TH signal is obtained when the laser is focused at the rear (i.e. right) boundary of the NL medium, the TH signal being ~7 times more intense as compared to the case where the focus is in the center of the NL medium. This could be related to the geometrical Gouy mismatch, as discussed in Section 2.4.

We can note in Fig. 4(b) that the output TH flux is almost the same for the front and rear focusing conditions, while the TH flux is minimum when the focus is located in the center.

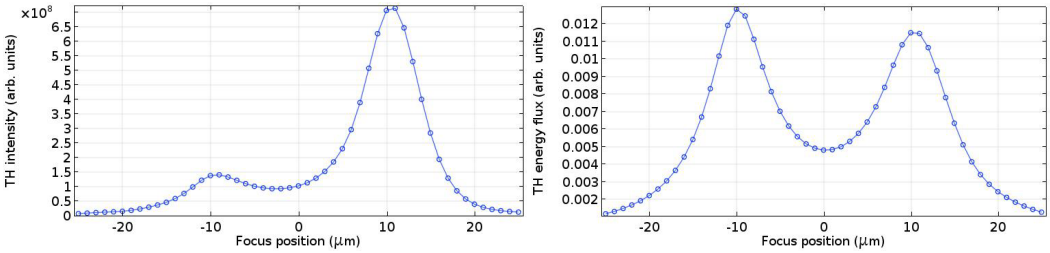

(a) (b)

Fig. 4. Intensity (a) and flux (b) of the TH radiation at the center of the rear boundary of the NL medium, as a function of focus position

The approximate equal TH flux for the front and rear focusing conditions could be related to the difference between the TH beam radius (and consequently to the divergence of the TH beam). Fig. 5(a) indicates that the divergence of the TH beam is very small when the F focusing is realized at the output boundary (see red curve in Fig. 5(a)).

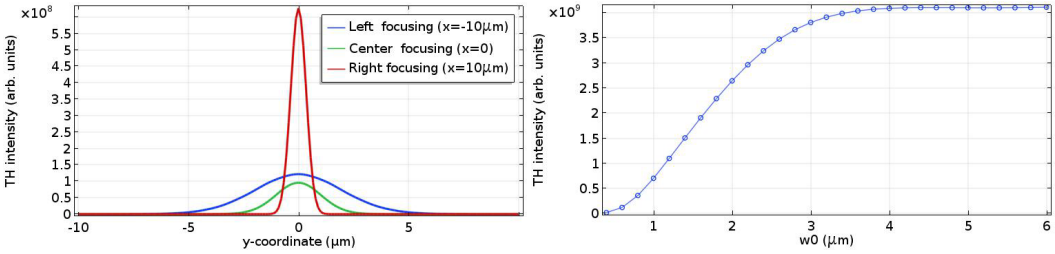

(a) (b)

Fig. 5. (a) Spatial intensity profile of the TH beam at the rear boundary for three focus positions. (b) TH intensity at the center of the output rear boundary as a function of beam waist radius.

For the case of optimum focusing conditions (i.e. F focusing at the rear boundary), we analyzed the influence of the beam waist w_0 on the TH intensity at the center of the output boundary. By keeping the intensity I_0 constant during the w_0 scan, we obtained the results presented in Fig. 5(b). One can note that the TH intensity increases rapidly with focus radius (for w_0 smaller than ~3 μm) and saturates at w_0 values larger than ~4 μm to a value that is approximately 5 times larger than that obtained for 1 μm radius. Thus, we obtain more than one order of

magnitude increase of the TH signal as compared to the case where 1 μm radius beam waist is located in the center of the NL medium, as presented in Fig. 4(a).

We further carried experiments on the TH signal intensity as a function of beam waist radius for two different F intensities: I_0= 10 and 14 TW/cm^2. For this, we focused IR (1064 nm wavelength) 5 ns laser pulses in open air [8] with three different focal-length lens: 3 cm, 5 cm and 10 cm. The beam waist radius in the experimental conditions presented here are ~3.5, 5.5 and 11 μm, respectively, while the Rayleigh length are ~70, 190 and 750 μm, respectively. The TH signal was analyzed in axial direction at ~10 cm away from the focus with a fibre-coupled spectrometer (Ocean Optics). In order to keep constant intensity in focus, we varied the pulse energy of the F pulses by changing the delay between the flash-lamp and Q-switch signals. The experimental data presented in Fig 6(a) (with errors in the 10% limit) indicate that TH signal intensity increase with F intensity: TH signal is higher at 14 TW/cm^2 as compared to 10 TW/cm^2. Fig. 6(a) also indicates that TH signal is stronger when using loose focusing conditions with 11 μm beam radius in focus.

As discussed in Section 2.4, this result can be understood as follows: when the beam radius increases, the length of focus (related to x_0) increases relative to the length L of the NL medium so that the interaction region is confined to a single geometrical coherence length, thus avoiding destructive phase cancellations.

The stronger TH signal obtained with loose focusing at high intensities is consistent with the numerical results presented in Fig. 6(b). The numerical data were obtained considering the NL medium as air ([10,13])), with L= 40 μm and h= 40 μm and the focus positioned in the center of the NL medium as in the experimental conditions. The good qualitative agreement of the numerical results with the experimental data validates the theoretical numerical model and the numerical calculation method presented here.

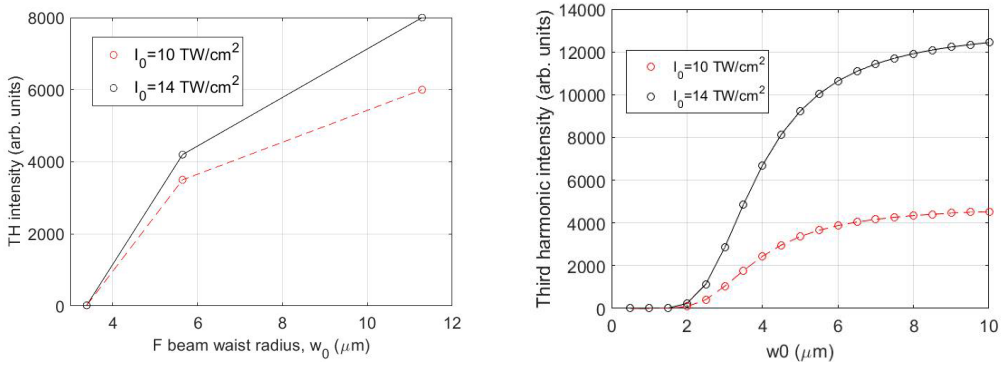

(a) (b)

Fig. 6. TH intensity vs F beam waist radius: (a) experimental data; (b) numerical results

5. Conclusions

In this paper we presented a theoretical study of the TH generation process in Xe and air induced by short nanosecond/ picosecond laser pulses.

We addressed analytically the influence of several factors on the THG process: the beam waist, the neutral gas and the plasma gas dispersions. We show than optimal (maximum) THG efficiency may be obtained by a suitable choice of the individual phase mismatches, geometrical mismatch which must be compensated by the neutral and the plasma gas dispersions, so that the total phase mismatch cancels.

We further addressed numerically the influence of the irradiation geometry on the efficiency of TH generation process with gaussian laser pulses. We found that the intensity of TH signal at the output of the NL medium can be increased by two alternative approaches: by focusing the driving laser radiation at the frontier of the NL medium, and by increasing the focal length (controlled by the driving beam waist radius) relative to the length of the NL medium. When the two methods are combined, we can boost the TH signal by more than one order of magnitude as compared to the case of non-optimized irradiation geometry condition. The theoretical results on the dependence of the TH signal to the driving beam waist radius are in good qualitative agreement with the experimental data: at a given driving intensity, the TH signal increase with beam radius and saturates when the focal length become much larger than the length of the NL medium.

Acknowledgment

This research was supported by the Ministry of Research, Innovation and Digitization (Ministerul Cercetării, Inovării și Digitalizării)/Institute of Atomic Physics from the National Research-Development and Innovation Plan III for 2015-2020/Programme 5/Subprograme 5.1 ELI-RO, project ELI-RO No ELI_13/16.10.2020.

R E F E R E N C E S

[1] *W. Boyd,* Nonlinear Optics, Academic Press Inc. 3rd Ed., Amsterdam, (2008).

[2]. *P. L. Shkolnikov, A. E. Kaplan, and A. Lago,* Phase-Matching Optimization of Large-Scale Nonlinear Frequency Upconversion in Neutral and Ionized Gases, J. Opt. Soc. Am. B, Vol. **13**, p. 412-443, (1996).

[3]. *Dejan B. Miloshevich, Suxing Hu, and Wilhelm Becker*, Quantum-mechanical model for ultrahigh-order harmonic generation in the moderately relativistic regime, Phys. Rev. A, Vol. **63**, p. 011403(R) (2001).

[4]. *J. Peatross, S. Voronov, and I. Prokopovich*, Selective Zoning of High Harmonic Emission Using Counter-Propagating Light, Optics Express,Vol. **1**, p. 114, (1997).

[5]. *C. Altucci, T. Starczewski, E. Mevel, C.-G. Wahlstrom, B. Carre, A. L'Huillier,* Influence of atomic density in high-order harmonic generation, J. Opt. Soc. Am. B, Vol. **13**, p. 148-157, (1996).
[6]. *Khoa Anh Tran, Khuong Ba Dinh, Peter Hannaford, and Lap Van Dao*, Phase-matched nonlinear wave-mixing processes in XUV region with multicolor lasers, Applied Optics, Vol. **58**, Issue 10, p. 2540-2545, https://doi.org/10.1364/AO.58.002540, (2019).
[7]. *J. B. Madsen, L. A. Hancock, S. L. Voronov, J. Peatross*, High-order harmonic generation in crossed laser beams, JOSA B, Vol. **20**, No. 1, p. 166-170, (2003).
[8]. *M. Stafe, C. Negutu, N. N. Puscas*, Third harmonic from air breakdown plasma induced by nanosecond laser pulses, Applied Physics B, Lasers and Optics, p. 105-109, (2018).
[9]. *P.W. Milonni and J.H. Eberly*, *Lasers*, Wiley, New York, (1988).
[10]. https://refractiveindex.info/?shelf=main&book=Xe&page=Bideau-Mehu
[11]. "COMSOL Multiphysics Reference Manual, version 5.3", COMSOL, Inc, www.comsol.com [12]. *M. Stafe,* Tree-step model for third-harmonic generation in air by nanosecond lasers, JOURNAL OF THE OPTICAL SOCIETY OF AMERICA B-OPTICAL PHYSICS 38 (7), pp.2206-2214 (2021).
[13]. . https://www.nist.gov/pml/atomic-spectra-database